


PREDICTION OF SOC IN CALCIC CHERNOZEM IN THE STEPPE ZONE OF UKRAINE USING BRIGHTNESS AND COLOUR INDICATORS

VADYM GORBAN ¹, ARTEM HUSLYSTYI¹, JOSÉ MANUEL RECIO ESPEJO², NATALIA BILOVA³

¹Department of Geobotany, Soil Science and Ecology, Faculty of Biology and Ecology, Oles Honchar Dnipro National University, Gagarin ave. 72, Dnipro, 49010, Ukraine; e-mail: gorvadym@gmail.com

²Department of Botany, Ecology and Plants Physiology, Faculty of Sciences, University of Córdoba, Campus Rabanales, Córdoba 14071, Spain

³Department of Hotel and Restaurant Services, Faculty of Innovative Technologies, University of Customs and Finance, Volodymyr Vernadsky st., 2/4, Dnipro, 49000, Ukraine

 Corresponding author

Received: 15 April 2021 / Accepted: 28 July 2021

Abstract

Gorban V., Huslysty A., Recio Espejo J. M., Bilova N.: Prediction of SOC in Calcic Chernozem in the steppe zone of Ukraine using brightness and colour indicators. *Ekológia (Bratislava)*, Vol. 40, No. 4, p. 325–336, 2021.

Soil organic carbon (SOC) is an important component of any soil which determines many of its properties. Nowadays, more and more attention is being paid to the SOC content determination in soils by not using the conventional, time-consuming and expensive technique, but by using colour image processing of soil samples. In this case, even the camera of modern smartphones can be used as an image source, making this technique very convenient and practical. However, it is important to maintain certain standardised conditions (light intensity, light incidence angle, etc.) when capturing the images of soil samples. In our opinion, it is best to use a regular scanner for this purpose, with subsequent image processing by graphic programs (e.g., Adobe Photoshop). To increase the reliability of the colour information obtained in this way, it is desired (if possible) to use a spectrograph or a monochromator in the subsequent calculation of reflection or brightness ratios. It is these two approaches that we have implemented in our work. As a result of the experiment, the values of brightness ratios (at 480, 650 and 750 nm wavelengths and integral brightness ratio), colour indicators (the hue, saturation and value [HSV], red, green and blue [RGB], CIE L*a*b* and cyan, magenta, yellow and key [CMYK] systems) and SOC content in Calcic Chernozem samples of the steppe zone of Ukraine were obtained. Using correlation analysis of the dataset, the existence of direct ($r = 0.88–0.90$) and inverse close relationships ($r = -0.75–0.90$) between SOC, values of brightness ratios and colour indicators of the soil samples were established. This allows us to develop predictive models. Statistical analysis showed that the models were significant when they were based on the values of brightness ratios at 650 nm wavelength, integral brightness ratio, V indicator in HSV system, R, G and B indicators in RGB system, C, M and K indicators in CMYK system and L* and b* indicators in L*a*b* system. The subsequent calculation of variation coefficients showed that the largest variability was observed in SOC indicators (CV = 0.72) and slightly less variability in the K index of CMYK system and brightness ratio values at 650 nm wavelength (CV = 0.67 and 0.53, respectively). Based on this, we believe that the models $y = 0.0188 + 0.0535 \cdot x$ (x is the value of the K index in CMYK system) and $y = 5.0716 - 3.2255 \cdot \log_{10}(x)$ (x is the value of brightness ratio at 650 nm wavelength) were the most statistically significant and promising parameters for determining SOC content (y in these equations) in Calcic Chernozem samples of the steppe zone of Ukraine.

Key words: brightness ratio, HSV, RGB, CMYK, L*a*b*, model.

Introduction

Nowadays, the world is experiencing an intensification of negative phenomena (desertification, aridisation, soil degradation, etc.) resulting in climate change (Borrelli et al., 2017; Li et al., 2020; Ma et al., 2020; Olifir et al., 2020). One of the main reasons for these processes is the global increase in ambient temperature as a result of an increase in greenhouse gas content in the atmosphere (Crowther et al., 2016; Dalal et al., 2021; Nahirniak et al., 2020).

As evidenced by studies (López-Díaz et al., 2017; Pechanec et al., 2018), soils are the main depot where carbon is being stored. In particular, the profile of ordinary Chernozems in the steppe zone of Ukraine contains 116–319 t/ha of soil organic carbon

(SOC; Baliuk et al., 2017). Specifically, SOC plays a crucial role in the global carbon cycle (Liang et al., 2017; Trigalet et al., 2016) and is also fundamental for the exhibition of soil fertility and ensuring its ecological functions by influencing its physical, chemical and biological properties (de Moraes Sá et al., 2018; Doetterl et al., 2015).

Extreme climate events with multiple occurrences cause significant changes in the state of ecosystems, which is accompanied by their degradation (Horion et al., 2019) and a decrease in the sequestration role; so, currently, there is a task to prevent humanity from crossing the critical border, beyond which global climate change will lead to catastrophic irreversible consequences globally (Chazdon, Brancalion, 2019). Thus, an assessment of carbon sequestration in different soils is required for the generation of

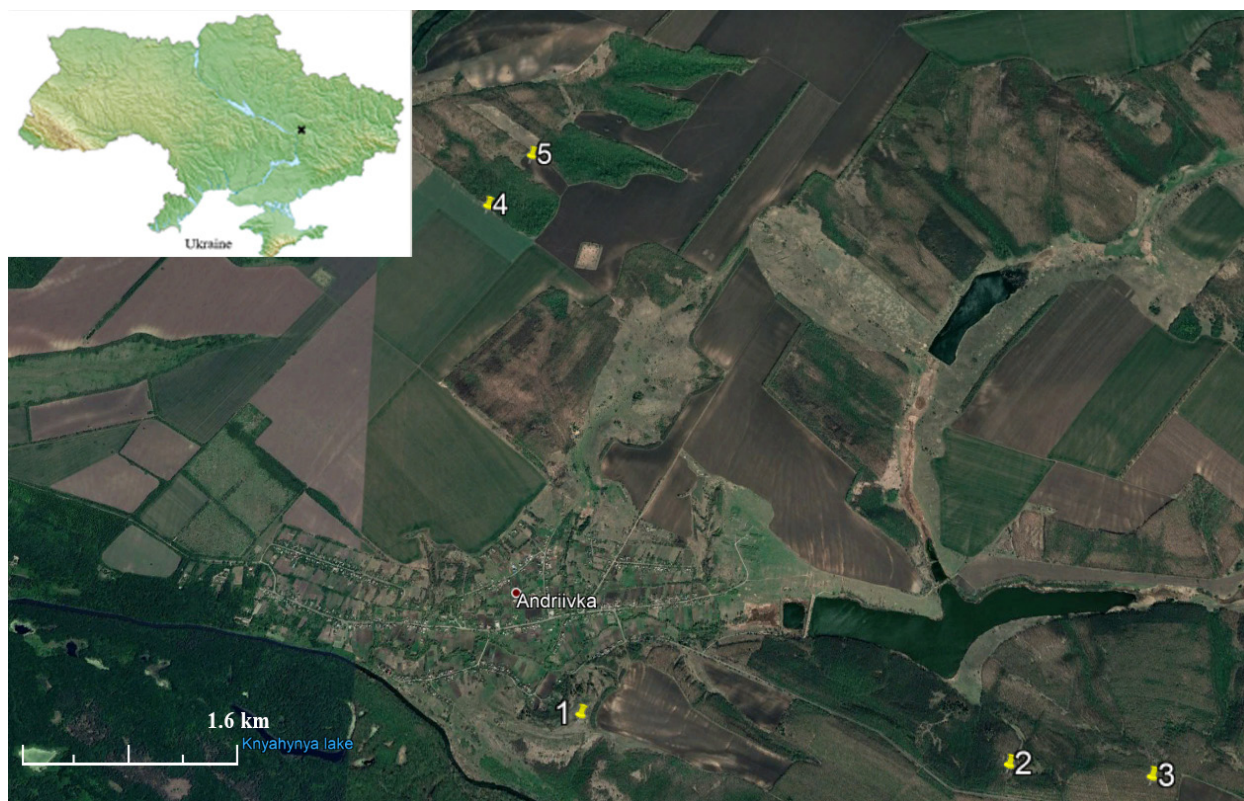


Fig. 1. Location of sites within the territory of the National Park 'Samarskiy Bir' (Novomoskovskiy district, Dnipropetrovsk Oblast, Ukraine).

sustainable development strategies in which humanity will strive to reduce the carbon content in the atmosphere by depositing it in the soils worldwide, which will help mitigate the effects of climate change (Rodríguez Martín et al., 2016).

Currently, the methods for soil properties assessment which can be applied on a large scale and in a short time are of particular importance. These requirements correspond to the methods for determining soil brightness and colour, results of which (after appropriate statistical processing) should be used for carbon content estimation in the soil (Fu et al., 2020; Gholizadeh et al., 2020). The soil colour can reflect its physical, chemical and biological properties and processes (Liu et al., 2020). It should be noted that the widely used Munsell colour chart has limited possibilities for assessing the soil colour due to its significant subjectivity. So, to perform a more objective determination of colour indicators, it is preferable to use diffuse reflectance spectroscopy (Torrent, Barrón, 2015) or a digital camera to subsequently determine the corresponding indicators in red, green and blue (RGB) system (Han et al., 2016; Kirillova et al., 2018; Levin et al., 2005). Moritsuka et al. (2014) noted the possibility of using CIE L*a*b* soil colour indicators to estimate the carbon, nitrogen and iron content in the topsoil. Studies conducted by Günal et al. (2007) and Liles et al. (2013) evidenced a relationship between the organic matter content and the saturation values of the L* soil colour, which is determined in the CIE L*a*b* system. Aitkenhead et al. (2013) found that the content of organic matter, nitrogen, calcium, titanium and molybdenum can be accurately predicted by colour using only the values of red, green and blue from the RGB system or L*, a* and b* from the CIE L*a*b* system. The results presented by Sánchez-Marañón et al. (2004) confirm the relationship between the saturation of the L* soil colour in CIE L*a*b* system and SOC con-

tent. Thus, colour indicators obtained in CIE L*a*b* system or RGB system are most often used to characterise the soil properties. The results of the study of soil brightness act as indicators that increase the reliability of the interpretation of data obtained in the study of soil colour indicators (Costa et al., 2020).

The purpose of our work is to study the feasibility of using brightness and colour indicators to estimate the SOC content in Calcic Chernozems of the steppe zone of Ukraine.

Material and methods

Site characteristics

Studies of colour parameters, reflectivity and carbon content in Calcic Chernozems were carried out on the territory of the National Park 'Samarskiy Bir' (Fig. 1) located in the southeastern part of the steppe zone of Ukraine (Novomoskovskiy district, Dnipropetrovsk Oblast, Ukraine).

Detailed descriptions of the sample plots and soil sections were presented in the works of Yakovenko (2017) and Gorban et al. (2020). Below, we give a brief description of the objects being studied using the mentioned works.

Site 1 was located within the virgin steppe land of a watershed plateau (48°45'36.9"N, 35°27'40.5"E). The herbaceous vegetative cover is closed, consisting of *Festuca valesiaca* Schleich. ex Gaudin, *Koeleria macrantha* (Ledeb.) Schult., *Thymus marschallianus* Willd., *Linum hirsutum* L., *Salvia nemorosa* L., *Artemisia austriaca* Jacq. and other herbaceous plant species. Soil profile description: A₁ (0–7 cm), A₂ (7–26 cm), Bk₁ (26–42 cm), Bk₂ (42–57 cm), Ck (57–120 cm+). The soil is Calcic Chernozem (IUSS, 2005).

Site 2 was located on the steppe virgin land; the area was represented by south-facing 3° slope (48°47'16.28"N, 35°27'17.17"E). The grass cover comprises *Festuca valesiaca* Goud. s.l., *Poa angustifolia* L., *Elytrigia repens* (L.) Nevski, *Poa nemoralis* L., *Lathyrus tuberosus* L., *Achillea millefolium* L., *Euphorbia vibrata* Waldst. et Kit., *Thymus marschallianus* Willd., *Linum hirsutum* L., *Agrimonia eupatoria* L., *Medicago romanica* Prod., *Melica transsilvanica* Schur and *Salvia nemorosa* L. Soil profile description: Ak (0–6 cm), Bk₁ (6–27 cm), Bk₂ (27–40 cm), Ck (40–120 cm+). The soil is Calcic Chernozem.

Site 3 was located on the steppe virgin land; the area was represented by north-facing 8° slope (48°47'14.93"N, 35°27'10.59"E). The vegetation cover contains *Prunus angustifolia* L., *Elymus repens* (L.) Nevski, *Achillea millefolium* L., *Salvia nemorosa* L., *Artemisia absinthium* L., *Euphorbia vibrata* Waldst. et Kit., *Galium aparine* L., *Viola odorata* L., *Lathyrus tuberosus* L. and *Convolvulus arvensis* L. Soil profile description: Ak₁ (0–8 cm), Ak₂ (8–23 cm), Bk₁ (23–51 cm), Bk₂ (51–80 cm), Ck (80–120 cm+). The soil is Calcic Chernozem (IUSS, 2005).

Site 4 was laid on the watershed plateau (48°45'27.6"N, 35°29'33.4"E). Forest stands were represented by *Robinia pseudoacacia* L., aged about 60 years. *Elymus repens* L., *Prunus angustifolia* L. and *Chelidonium majus* L. predominate in the herbaceous cover, with a total coverage of about 60%–70%. Soil profile description: A (0–14 cm), B (14–34 cm), Bk (34–56 cm), Ck (56–120 cm+). The soil is Calcic Chernozem.

Site 5 was located on a watershed plateau next to Site 4 (48°45'27.0"N, 35°30'09.5"E). Forest stand is represented by *Quercus robur* L., aged about 60 years. In the herbaceous cover, *Elymus repens* L., *Verbascum lychnitis* L., *Salvia verticillata* L. and *Ajuga genevensis* L. predominate, with a total coverage of about 20%–25%. Soil profile description: A₁ (0–9 cm), A₂ (9–42 cm), Bk₁ (42–62 cm), Bk₂ (62–81 cm), Ck (81–120 cm+). The soil is Calcic Chernozem (IUSS, 2005).

A detailed description of the physical, chemical and micro-morphological properties of the Calcic Chernozem studied in the steppe zone of Ukraine was presented in our previous works (Bilova, Travleev, 1999; Bozhko, Bilova, 2020; Gorban, 2019; Gorban, Boloban, 2019; Gorban et al., 2020; Recio Espejo et al., 2020, etc.).

Sample procedures

About 1 kg of composite sample soil was collected at each of the five sites in the summer of 2016. Samples were taken from the middle of each genetic horizon. The selected soil samples were then used to determine the colour parameters, reflectivity and carbon content in the laboratory settings.

Laboratory analyses

Field description of soil profiles was carried out according to the guidelines for soil description (2006). The classification position of the studied soils was determined as per the International Union of Soil Sciences Working Group on the World Reference Base 2015. The classification position of the studied soils was determined as per the IUSS Working Group WRB 2015. For laboratory studies, air-dried soil samples were used.

The brightness was determined using a monochromator within the range of wavelength 400–750 nm by determining the spectral brightness ratios reflected as the percentage ratio of the

brightness of the object studied to the brightness of a white surface (reference). The source of the radiation was a halogen lamp. For the study, a soil fraction of 0.5–1.0 Ø mm was used. The sample was placed in a quartz cuvette 35×17×5 mm. Analytically pure magnesium oxide was used as a reference. The reflectivity was measured in 5-nm increments averaging over three values at each point for each wavelength value. The obtained reflectivity values at certain wavelengths were used to plot a diagram with OriginPro 9.1 software to calculate the values of the brightness ratios at 480, 650 and 750 nm wavelengths, as well as the integral brightness ratio according to the principle described in Orlov et al. (2001).

Determination of the soil colour was performed using a scanner. For scanning, soil samples used were previously moistened to a pasty state, mixed, placed in special rounded moulds with a size of approximately 25×25 mm and dried on the glass to an air-dry state. Part of the sample was moistened before placing it on the scanner glass. This allowed measuring the characteristics of dry and wet samples in a single run (Gorban et al., 2019). In the subsequent analysis of the captured image, Adobe Photoshop eyedropper tool (5×5 pixels) with 300 pixels resolution was applied; it allows obtaining a range of colour characteristics of the object in hue, saturation and value (HSV), RGB, CIE L*a*b* and cyan, magenta, yellow and key (CMYK) colour models commonly used in soil colour characterisation (Simón et al., 2020).

Organic carbon in the soil was determined by the oxidimetric method. Soil organic matter was oxidised by a solution of potassium dichromate (K₂Cr₂O₇) at a temperature of 140°C–150°C, followed by quantitative determination of the portion that was unreacted with Mohr's salt ((NH₄)₂SO₄·FeSO₄·6H₂O) (Carter, Gregorich, 2008).

Statistical analysis

Data analysis was performed in Statistica 12.0 package (StatSoft Inc., USA) and the Analysis ToolPak in Microsoft Excel (Microsoft Corporation). The model predictive ability and stability were evaluated by comparing R² (the coefficient of determination) and root mean square error (RMSE). R² indicator was used to test the stability, and RMSE indicator was used to test the predictive ability of the model (Fu et al., 2020). The ideal model should have a high R² and a low RMSE, indicating that the model is more stable and accurate (Wu et al., 2017). RMSE can be expressed as follows:

$$RMSE = \sqrt{\frac{\sum_{i=1}^n (SOM_{pre} - SOM_{mea})^2}{n}} \quad (1)$$

where SOM_{pre} is the predicted SOM, SOM_{mea} is the measured SOM and n is the sample number. Performance of the model was estimated by the coefficient of determination (R²), the RMSE (equation 1) and the ratio of performance to deviation (RPD; equation 2).

$$RPD = \frac{SD}{RMSE} \quad (2)$$

where SD is the standard deviation of the measured SOM values. In the study, we followed the RPD classification proposed by Chang and Laird (2002). Models having RPD >2 were considered to be good quantitative models.

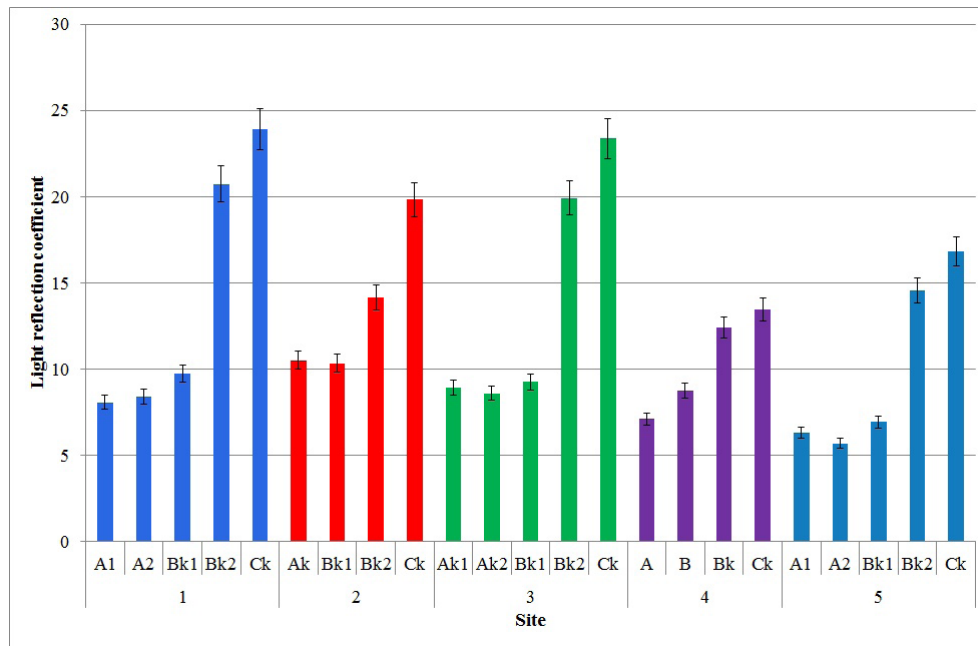


Fig. 2. The brightness ratio of Calcic Chernozem samples at 480 nm wavelength.

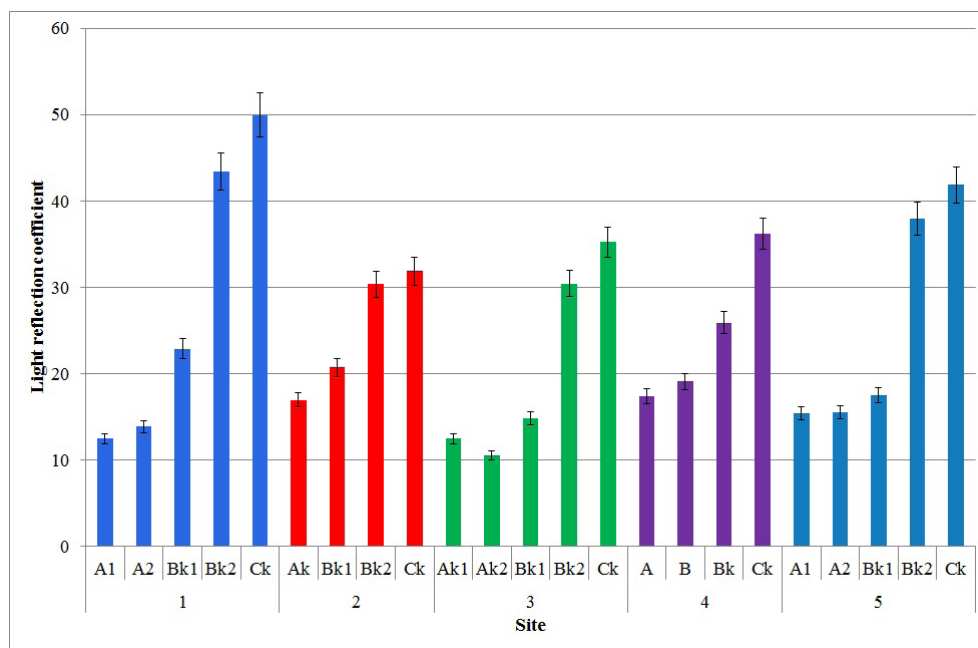


Fig. 3. The brightness ratio of Calcic Chernozem samples at 750 nm wavelength.

Results

The brightness of the studied soils

Orlov et al. (2001) noted that the values of brightness ratio at 480, 650 and 750 nm wavelengths, as well as the integral brightness ratio are most often used to characterise the soil organic matter content. Since this is exactly the goal in our work, we also used these brightness ratios.

Analysis of the brightness coefficient values of Calcic Chernozem samples of Site 1 at 480 nm wavelength showed that the sample taken from the A₁ horizon (8.07) had the lowest value. In the samples taken from A₂ and Bk₁ horizons, a gradual increase in the brightness ratio value was observed, and from the sample taken from Bk₂ horizon, this increase was sharp; the maximum value (23.89) was reached in the sample taken from Ck horizon. A similar pattern of changes in the coefficient values was observed for the soil samples taken from other sample sites (Fig. 2).

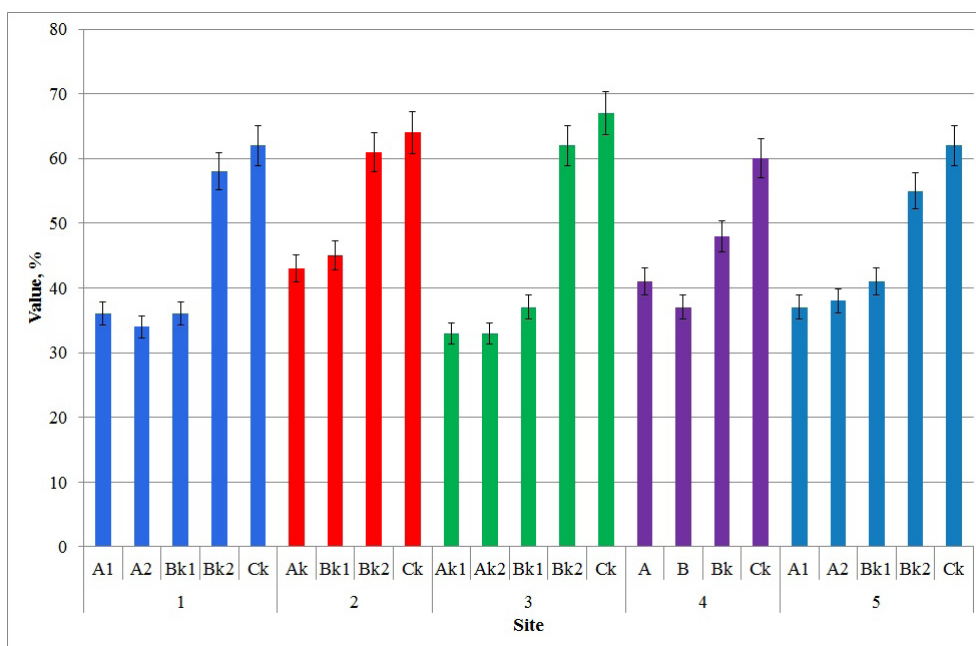


Fig. 4. The V index (HSV system) of Calcic Chernozem samples.

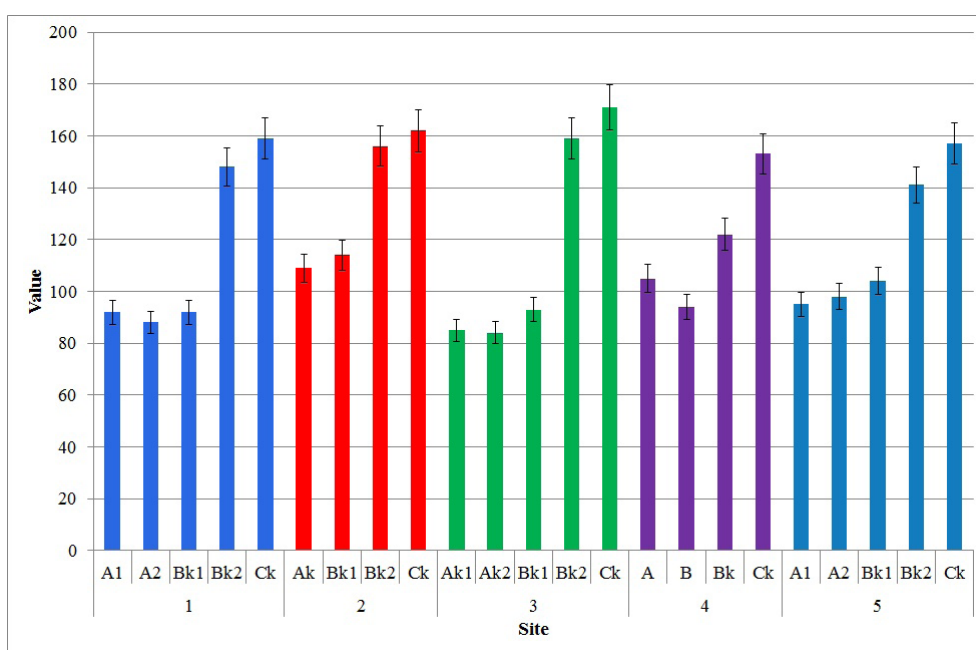


Fig. 5. Values of the R index (RGB system) of Calcic Chernozem samples.

However, under conditions of sites 2, 3 and 5, a decrease in the brightness ratio was observed in the soil samples taken from the second horizon compared to the ones from the first horizon. This can be explained by significant enrichment of the first horizons with the root residues mainly removed from the soil sample during its preparation for laboratory analysis, but even their insignificant content can significantly increase the brightness values of the samples taken from the first horizons of the studied soils.

The results of determining the brightness ratio of Calcic Chernozem samples of Site 1 at 650 nm wavelength revealed that its minimum values were characteristic of the sample taken from the A₁ horizon (9.57). With increasing depth, an increase in the values of the brightness ratio was observed; moreover, from the Bk₂ horizon, it was sharp. The Calcic Chernozem samples taken from other sample sites were characterised by similar features of changes in brightness ratio values with depth, but the samples from the second horizons of sites 3 and 5 were different in lower

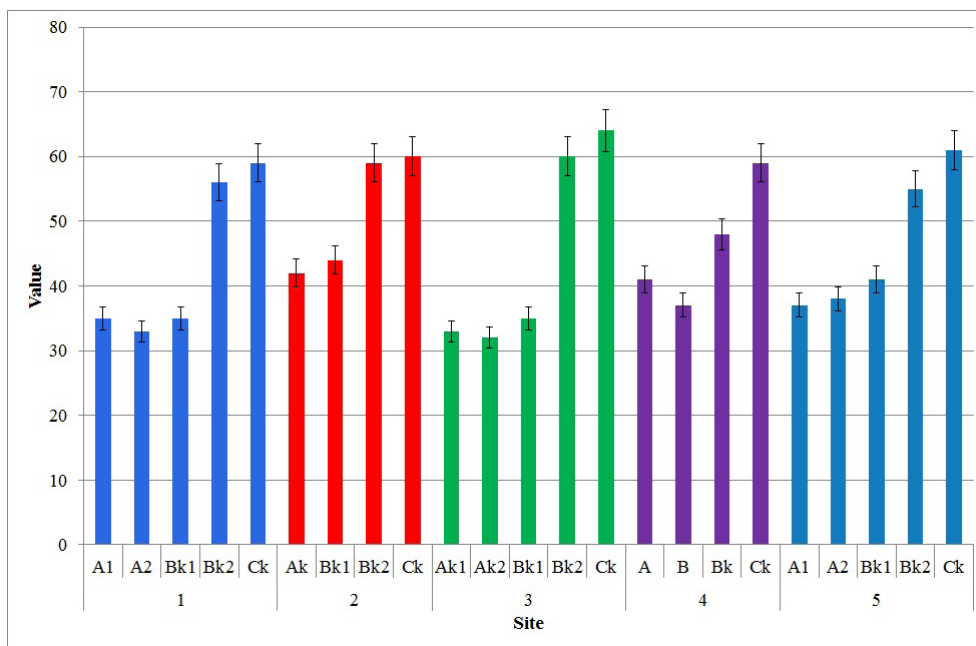


Fig. 6. Values of the L* index (L*a*b* system) of Calcic Chernozem samples.

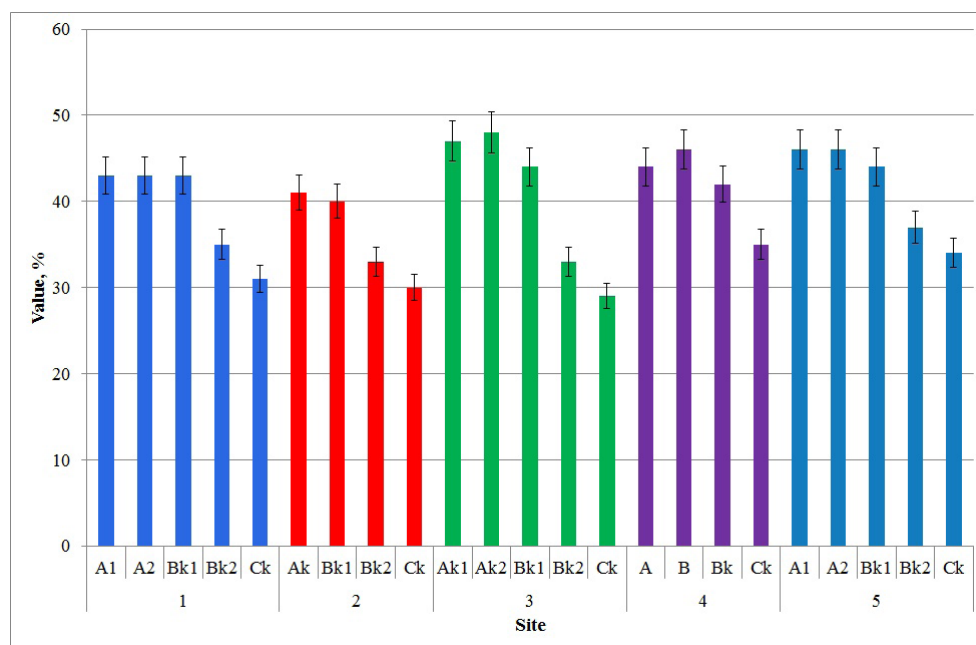


Fig. 7. Values of the C index (CMYK system) of Calcic Chernozem samples.

brightness ratio values compared to the samples from the first ones.

Changes in the brightness ratio at 750 nm wavelength (Fig. 3) and the integral brightness ratio of Calcic Chernozem samples were similar. Minimum values of these coefficients were typical for samples of the upper horizons, and their increase with depth was observed. In this case, the Calcic Chernozem sample from the A₂ horizon of Site 5 was characterised by smaller values of these ratios compared to the sample from the A₁ horizon.

Colour indicators of the studied soils

Currently, many researchers noted significant subjectivity of the Munsell colour chart application in determining the soil colour (Kirillova et al., 2018; Ramos et al., 2020). Standardised use of a variety of methods and sensors is becoming increasingly common for this purpose (Swetha, Chakraborty, 2021; Taneja et al., 2021). In our opinion, one of these methods is the colour determination in the soil sample using a conventional scanner. This

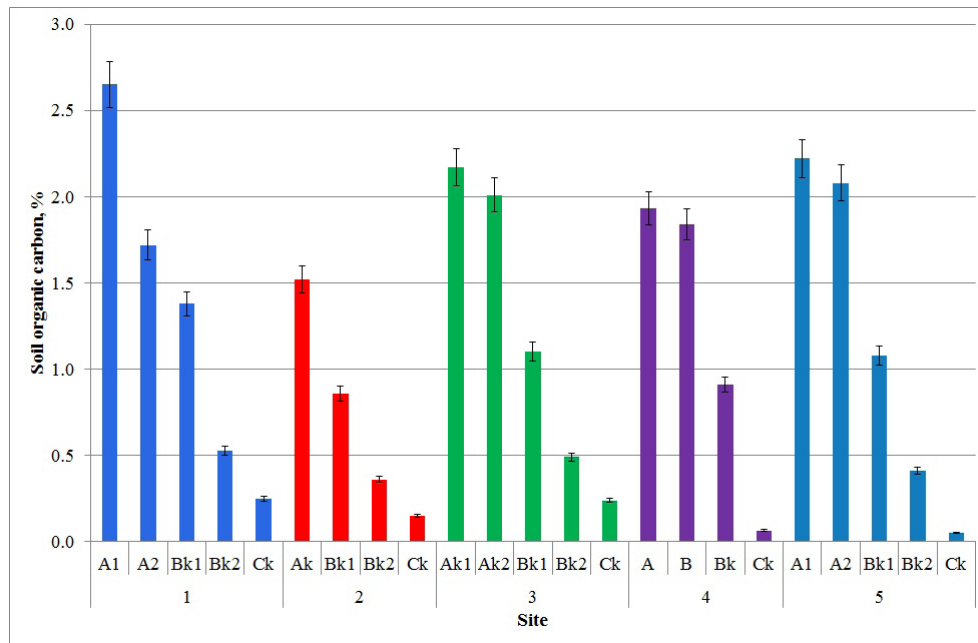


Fig. 8. SOC content in Calcic Chernozem samples.

method provides fast acquisition of a large dataset under standardised conditions (Gorban et al., 2019).

Analysis of the colour characteristics of soil samples in the HSV model showed that the lowest values of H (hue), S (saturation) and V (value) were typical for the samples taken from the two upper horizons. The soil sample taken from the Bk₁ horizon of the sample site differed in smaller H and S values compared to the sample from the A₂ horizon, and sample from the A₂ horizon also differed in smaller V values (Fig. 4) than the sample taken from A₁ horizon. In Site 2, the sample taken from the Bk₁ horizon differed in smaller S and V values compared to the sample taken from the Ak horizon. In Site 5, the sample taken from the A₂ horizon differed in smaller H and S values than the sample taken from the A₁ horizon. In other cases, a decrease in the H, S and V values was observed with an increase in sampling depth.

Analysis of the colour characteristics of soil samples in the RGB system established that the lowest values of the R (red), G (green) and B (blue) indexes were mainly typical for the samples taken from the first upper horizons. However, the sample from the A₂ horizon of Site 1 differed in smaller values of the R, G and B indexes (88, 76 and 65, respectively) compared to those of a sample taken from the A₁ horizon (92, 79 and 70, respectively). The same feature was observed for samples from Site 2: the sample taken from the Bk₂ horizon differed in smaller values of the R, G and B indexes than the values of the sample taken from the Ak horizon. The sample taken from the A₂ horizon of Site 5 was characterised by lower values of the R and G indexes compared to the sample from the A₁ horizon (Fig. 5).

The L* index (lightness) was the most informative indicator among the indicators of the L*a*b* system. In general, Calcic Chernozem samples taken from deeper horizons correspond to higher values of the L* index (Fig. 6). However, the samples taken from the A₁ horizon of Site 1, Bk₁ horizon of Site 2 and A₂ horizon of Site 3 differed by showing lower values of the L* index

compared to the samples taken from the overlying horizons of the corresponding sites.

In the CMYK system, C (cyan), M (magenta) and K (key) colour indicators most accurately reflect the features of colour changes in soil samples; values of the indicators gradually decreased with depth (Fig. 7). At the same time, the values of the Y (yellow) indicator of the soil samples changed slightly and were within the range of 60–67. At the same time, the sample taken from the Bk₂ horizon of Site 2 differed in large values of the C, M and K indicators (46, 52 and 33%, respectively) compared to the sample of Ak horizon (44, 51 and 27%, respectively).

SOC content in the studied soils

Soil is a major pool of organic carbon (Fontaine et al., 2007), which strongly interacts with atmospheric composition, climate and land cover change. So, the ability to predict and mitigate the global change effects depends on understanding the SOC distribution and control in soil (Jobbágy, Jackson, 2000; Rodríguez Martín et al., 2016). Based on this, currently, monitoring of SOC content in the soil is an urgent global task on which the subsequent development of global climate changes caused by an increase in the content of atmospheric greenhouse gases depends.

As a result of the analyses performed, it was observed that the maximum SOC content (2.65%) was found in the A₁ horizon of Site 1 (Fig. 8). A sharp decrease in SOC content was observed with increasing depth, and its content in the Ck horizon was only 0.25%. The highest SOC in the soil of Site 2 was found in the Ak and Bk₁ horizons (1.93 and 1.84%, respectively). In the soils of sites 3 and 5, the highest SOC content was also associated with the two upper (topsoil) horizons. A horizon of Site 4 was characterised by a significantly higher SOC compared to other horizons.

Table 1. Correlation coefficients between SOC content, the values of brightness ratio and colour indicators in the investigated soil samples of Calcic Chernozem.

	SOC	ρ_{480}	ρ_{650}	ρ_{750}	ρ_{Σ}	H, °	S, %	V, %	R	G	B	L	a	b	C, %	M, %	Y, %	K, %
SOC	1.00																	
ρ_{480}	-0.79	1.00																
ρ_{650}	-0.87	0.98	1.00															
ρ_{750}	-0.86	0.97	0.99	1.00														
ρ_{Σ}	-0.86	0.98	1.00	0.99	1.00													
H, °	-0.75	0.79	0.79	0.78	0.80	1.00												
S, %	-0.80	0.65	0.76	0.76	0.74	0.70	1.00											
V, %	-0.90	0.83	0.91	0.89	0.91	0.81	0.84	1.00										
R	-0.90	0.83	0.91	0.89	0.91	0.81	0.84	1.00	1.00									
G	-0.90	0.85	0.92	0.90	0.92	0.83	0.81	1.00	1.00	1.00								
B	-0.88	0.84	0.91	0.88	0.91	0.82	0.76	0.99	0.99	1.00	1.00							
L*	-0.90	0.84	0.91	0.89	0.92	0.84	0.82	1.00	1.00	1.00	0.99	1.00						
a*	-0.59	0.38	0.53	0.54	0.50	0.28	0.82	0.68	0.68	0.63	0.58	0.63	1.00					
b*	-0.89	0.78	0.88	0.87	0.87	0.82	0.93	0.98	0.98	0.97	0.94	0.97	0.74	1.00				
C, %	0.88	-0.77	-0.87	-0.86	-0.86	-0.73	-0.93	-0.97	-0.97	-0.95	-0.92	-0.95	-0.81	-0.98	1.00			
M, %	0.88	-0.86	-0.92	-0.89	-0.93	-0.86	-0.77	-0.98	-0.98	-0.99	-0.99	-0.99	-0.55	-0.94	0.92	1.00		
Y, %	0.34	-0.41	-0.44	-0.38	-0.46	-0.10	-0.02	-0.46	-0.46	-0.48	-0.54	-0.46	-0.20	-0.29	0.36	0.50	1.00	
K, %	0.90	-0.85	-0.91	-0.90	-0.92	-0.85	-0.81	-0.99	-0.99	-1.00	-0.99	-1.00	-0.61	-0.96	0.94	0.99	0.44	1.00

Note: The noted correlations were significant at the level $p < 0.05000$, $n = 23$.

Relationship between brightness, colour parameters and SOC in the studied soils

Currently, many researchers have shown the ability to determine the SOC content in the soil, not in a conventional, time-consuming and expensive way, but by using the information on the brightness and colour of soil samples, taking into account the existing relationships between the data on soil characteristics (Fu et al., 2020; Morellos et al., 2016; Zhou et al., 2020).

To determine the existing relationships between the SOC content in soil samples, their brightness and colour characteristics, we performed a correlation analysis of the obtained dataset, the results of which are presented in Table 1.

The data analysis showed a close inverse relationship between the SOC content in soil samples and the values of the brightness ratios at 480, 650 and 750 nm wavelengths, integral brightness ratio, the H, S and V indicators (HSV system), the R, G and B indicators (RGB system) and the C and Y indicators (CMYK system). A direct close relationship was found between the SOC content in soil samples and the values of the L* and b* indicators (L*a*b* system) and the K indicator (CMYK system). Based on the data obtained, it can be assumed that almost all the indicators that were considered above in the work can be used to model the SOC content in soil samples.

The results of modelling based on regression analysis are presented in Table 2. Taking into account information about the parameters of the models (R^2 , RMSE, RPD) characterised in the works of Wu et al. (2017) and Fu et al. (2020), we can conclude that the models with the following parameters are successful: $R^2 > 0.75$; RMSE < 0.50; RPD > 2.00. In our case, models for SOC content determination in soil samples are statistically reliable based

on the use of brightness ratios with 650 and 750 nm wavelengths, integral brightness ratio, the V indicator (HSV system), the R, G and B indicators (RGB system), the C, M and K indicators (CMYK system) and the L* and b* indicators (L*a*b*system).

Additionally, coefficients of variation (CVs) of the SOC content values in the soil samples and their brightness values and colour characteristics were calculated. As a result, it turned out that the highest CV was characteristic of the SOC content values (CV = 0.72). A slightly lower CV was found in the K index values (CMYK system), brightness ratio at 650 nm wavelength, integral brightness ratio and brightness ratio at 750 nm wavelength (CV values were 0.67, 0.53, 0.50 and 0.46, respectively). For this reason, the K index values (Fig. 9a) and brightness ratio at 650 nm wavelength (Fig. 9b) give the best fit to predict the SOC content in Calcic Chernozem samples.

Discussion

The Calcic Chernozem samples taken from the upper horizons of all sample sites were characterised by lower values of the brightness ratio (at 480, 650 and 750 nm wavelengths and integral brightness ratio) compared to the samples taken from the lower horizons. At the same time, the samples taken from the Bk₂ and Ck lower horizons of sites 1, 2, 3 and 5 were characterised by a sharp increase in brightness ratio values compared to the samples taken from the deeper horizons, which may indicate a sharp SOC content decrease in the samples from these horizons. The samples taken from Site 4 were characterised by a gradual increase in brightness ratio values with depth, that is, it can be assumed that SOC gradually decreased in this soil from A to Ck horizon.

Table 2. Modelling of the SOC content (%) in Calcic Chernozem based on brightness and colour indicators (y – SOC content; x – colour brightness indicator).

Indicator (x)	Equation	R ²	RMSE	RPD
p480	$y = 2.5597 - 0.1141 \cdot x$	0.62	0.50	1.65
p650	$y = 5.0716 - 3.2255 \cdot \log_{10}(x)$	0.81	0.35	2.33
p750	$y = 4.0819 - 0.1826 \cdot x + 0.0021 \cdot x^2$	0.83	0.33	2.48
pΣ	$y = 3.7807 - 0.2471 \cdot x + 0.0043 \cdot x^2$	0.81	0.35	2.33
H, °	$y = -1.7918 + 0.3707 \cdot x - 0.0089 \cdot x^2$	0.64	0.48	1.69
S, %	$y = 4.838 - 0.1433 \cdot x$	0.64	0.48	1.72
V, %	$y = 4.052 - 0.0616 \cdot x$	0.82	0.34	2.40
R	$y = 4.0444 - 0.0241 \cdot x$	0.81	0.35	2.34
G	$y = 4.0984 - 0.0281 \cdot x$	0.81	0.35	2.33
B	$y = 4.7328 - 0.0407 \cdot x$	0.78	0.38	2.18
L*	$y = 4.1502 - 0.0653 \cdot x$	0.81	0.35	2.37
a*	$y = 3.1119 - 0.2978 \cdot x$	0.34	0.65	1.26
b*	$y = 2.9586 - 0.133 \cdot x$	0.80	0.36	2.27
C, %	$y = -3.6248 + 0.1197 \cdot x$	0.77	0.39	2.13
M, %	$y = -4.6284 + 0.1189 \cdot x$	0.78	0.38	2.16
Y, %	$y = -4.9731 + 0.0933 \cdot x$	0.12	0.75	1.09
K, %	$y = 0.0188 + 0.0535 \cdot x$	0.82	0.34	2.40

The values of the HSV system parameters of the studied Calcic Chernozem samples increased with increasing depth of their sampling. At the same time, a sharp increase in the values of the H and V indicators in the samples taken from the lower B_k and C_k horizons was observed in sites 1, 2, 3 and 5, as well as in the samples taken from B_k and C_k horizons of Site 4. This may indicate a sharp decrease in SOC content of the samples taken from the lower horizons of all the studied soils. In terms of the H value, the samples of the two upper horizons of all the sample sites practically did not differ from each other.

A significant increase in the values of the RGB and L*a*b* systems was also typical for the samples taken from the lower horizons of all sample sites; it may indicate that these parameters can be used for SOC content identification in the samples of Calcic Chernozem.

Values of the C, M and Y indicators of the CMYK system obtained for samples taken from the two upper horizons of all the sample sites had much in common with each other. In general, the samples taken from the upper horizons differed in large values of the indicators of this system in comparison with the samples taken from the lower horizons.

The maximum SOC content was found in the samples taken from the upper horizons of all the studied soils. The samples taken from the lower horizons of sites 1, 2, 3 and 5 were characterised by a sharp decrease in the SOC content compared to the upper horizons. In samples of Site 4, a gradual decrease in the SOC content was observed with an increase in the depth of sampling.

Correlation analysis of the obtained result dataset showed direct and inverse close relationships between the values of brightness ratio, colour indicators and SOC content in the studied Calcic Chernozem samples. This became the rationale for the creation of models, the use of which will help in the calculation of SOC content in Calcic Chernozem samples from the values of brightness ratio and colour indicators.

Analysis of the obtained models showed a possibility of using the brightness ratio values at 650 nm ($y = 5.0716 - 3.2255 \cdot \log_{10}(x)$) and 750 nm ($y = 4.0819 - 0.1826 \cdot x + 0.0021 \cdot x^2$) wavelengths, integral brightness ratio ($y = 3.7807 - 0.2471 \cdot x + 0.0043 \cdot x^2$), the V indicator of the HSV system ($y = 4.052 - 0.0616 \cdot x$), the R, G and B indicators of the RGB system ($y = 4.0444 - 0.0241 \cdot x$, $y = 4.0984 - 0.0281 \cdot x$ and $y = 4.7328 - 0.0407 \cdot x$, respectively), the C, M and K indicators of the CMYK system ($y = -3.6248 + 0.1197 \cdot x$, $y = -4.6284 + 0.1189 \cdot x$ and $y = 0.0188 + 0.0535 \cdot x$, respectively) and the L* and b* indicators of the L*a*b* system ($y = 4.1502 - 0.0653 \cdot x$ and $y = 2.9586 - 0.133 \cdot x$, respectively). In all the models presented, x is the value of the corresponding brightness ratio or colour indicator and y is SOC content. All models were characterised by R² values from 0.75 to 0.83, RMSE from 0.33 to 0.39 and RPD from 2.13 to 2.48, which indicates the possibility of their practical application.

Calculation of CVs of all the studied characteristics showed that the largest variability was characteristic of SOC content in the samples. Among the brightness ratio and colour indicators, the largest variability was characteristic of the K index values of the CMYK system and the brightness ratio values at 650 nm wavelength. Therefore, these two characteristics are best suited for calculating SOC content in Calcic Chernozem samples.

Conclusion

The samples taken from the upper horizons of Calcic Chernozem under study were characterised by lower values of brightness ratio at 480, 650 and 750 nm wavelengths as well as integral brightness ratio than the values of the lower horizons. At the same time, a sharp increase in these indicators was typical for the samples taken from the lower B_k and C_k soil horizons of sites 1, 2, 3 and 5. In general, a similar distribution of the values of the colour

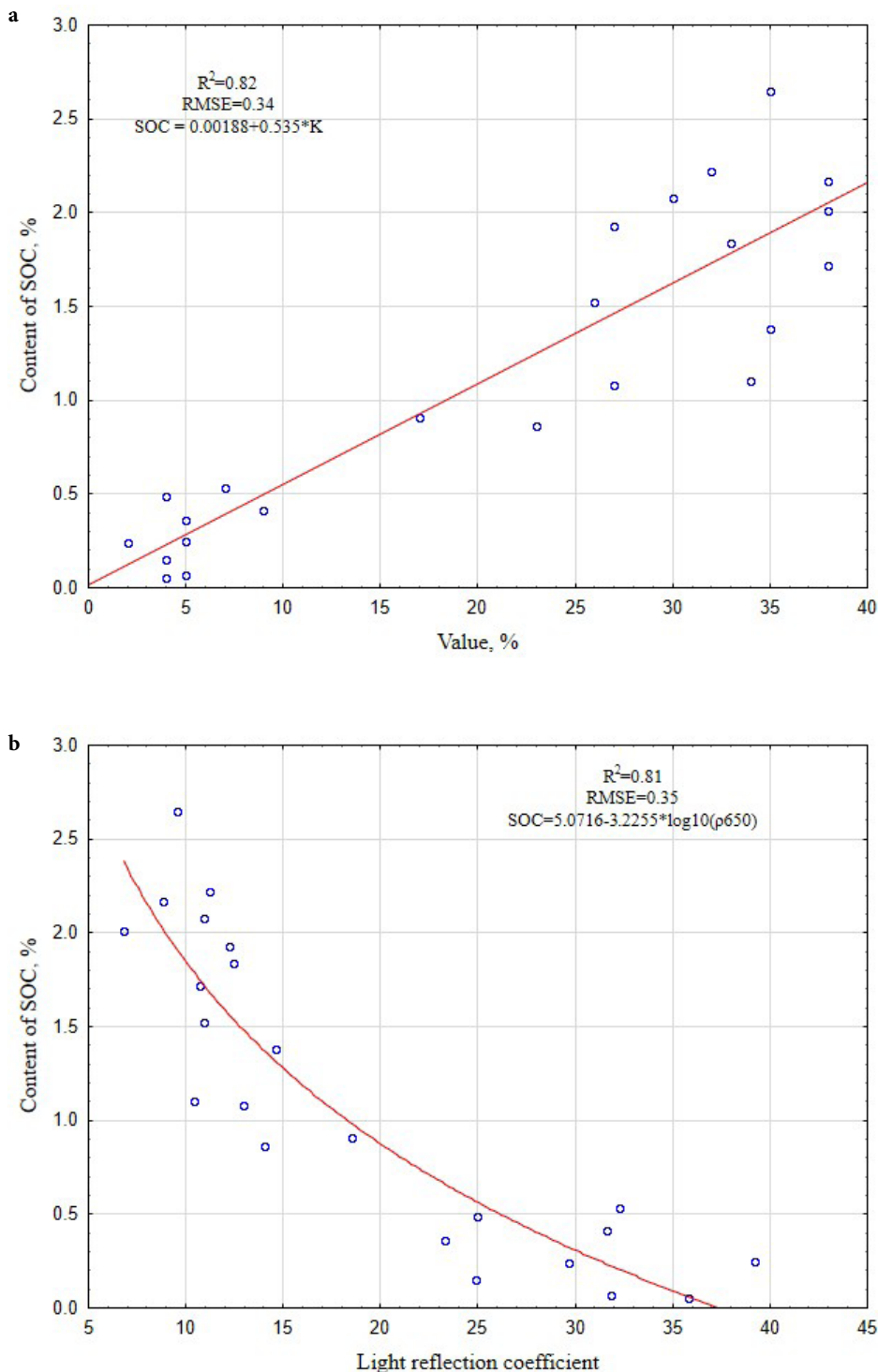


Fig. 9. Diagram of SOC content in Calcic Chernozem samples, dependent on the K index value of the CMYK system (a) and on the brightness ratio value at 650 nm wavelength (b).

indicators of the HSV, RGB and L*a*b* systems was found for all the studied soil samples. The samples taken from the upper horizons of all the studied soils were characterised by increased CMYK system indicators in comparison with the samples from the lower horizons. SOC content analysis in the studied samples

showed its significant accumulation in the upper soil horizons with a sharp decrease in its content with depth. The correlation analysis performed showed direct and inverse close relationships between the studied indicators, which made it possible to develop the models for SOC calculation in soil samples using the

values of brightness ratio and colour indicators. As a result, it was found that the models using values of brightness ratio at 650 nm wavelength, integral brightness ratio, the V indicator of the HSV system, the R, G and B indicators of the RGB system, the C, M and K indicators of the CMYK system and the L* and b* indicators of the L*a*b* system (x is the value of the corresponding brightness ratio or colour indicator, y is SOC content) were statistically significant. The calculation of CVs showed that the largest variability was observed in SOC content indicators; it was slightly less in the K index of the CMYK system and the brightness ratio index at 650 nm wavelength. That is why, we believe that the models $y = 0.0188 + 0.0535 \times x$ (x is the value of the K index of the CMYK system) and $y = 5.0716 - 3.2255 \times \log_{10}(x)$ (x is the value of the brightness ratio at 650 nm wavelength) were the most promising for SOC content determination (y in these equations) in Calcic Chernozem samples of the steppe zone of Ukraine.

References

- Aitkenhead, M.J., Coull, M., Towers, W., Hudson, G. & Black H.I.J. (2013). Prediction of soil characteristics and colour using data from the National Soils Inventory of Scotland. *Geoderma*, 200–201, 99–107. DOI: 10.1016/j.geoderma.2013.02.013.
- Baliuk, S., Medvediev, V., Kucher, A., Solovej, V., Levin, A. & Kolmaz J. (2017). Control over organic carbon of soil in a context of food safety and climate fluctuation (in Ukrainian). *Visnyk Agrarnoi Nauky*, 95(9), 11–18. DOI: 10.31073/agrovisnyk201709-02.
- Bilova, N.A. & Travleev A.P. (1999). *Natural forest and grassland soils (in Russian)*. Dnepropetrovsk: DNU.
- Borrelli, P., Robinson, D. A., Fleischer, L. R., Lugato, E., Ballabio, C., Alewell, C., Meusburger, K., Modugno, S., Schütt, B., Ferro, V., Bagarello, V., Oost, K.V., Montanarella, L. & Panagos P. (2017). An assessment of the global impact of 21st century land use change on soil erosion. *Nature Communications*, 8(1). DOI: 10.1038/s41467-017-02142-7.
- Bozhko, K. & Bilova N. (2020). The influence of the slope exposure on the soil aggregation and structure, water stability of aggregates, and ecological microstructure formation of the ravine forest soils in Pre-Dnipro Region (Ukraine). *Ekológia (Bratislava)*, 39(2), 116–129. DOI: 10.2478/eko-2020-0009.
- Carter, M.R. & Gregorich E.G. (2008). *Soil sampling and methods of analysis*. Boca Raton: CRC Press.
- Chang, C.-W. & Laird D.A. (2002). Near-infrared reflectance spectroscopic analysis of soil C and N. *Soil Sci.*, 167(2), 110–116. DOI: 10.1097/00010694-200202000-00003.
- Chazdon, R. & Brancalion P. (2019). Restoring forests as a means to many ends. *Science*, 365(6448), 24–25. DOI: 10.1126/science.aax9539.
- Costa, J.J.F., Giasson, E., da Silva, E.B., Coblinski, J.A. & Tiecher T. (2020). Use of color parameters in the grouping of soil samples produces more accurate predictions of soil texture and soil organic carbon. *Comput. Electron. Agric.*, 177, 105710. DOI: 10.1016/j.compag.2020.105710.
- Crowther, T.W., Todd-Brown, K.E.O., Rowe, C.W., Wieder, W.R., Carey, J.C., MacHmuller, M.B., Snoek, B.L., Fang, S., Zhou, G., Allison, S.D., Blair, J.M., Bridgman, S.D., Burton, A.J., Carrillo, Y., Reich, P.B., Clark, J.S., Classen, A.T., Dijkstra, F.A., Elberling, B., Emmett, B.A., Estiarte, M., Frey, S.D., Guo, J., Harte, J., Jiang, L., Johnson, B.R., Kroël-Dulay, G., Larsen, K.S., Laudon, H., Lavellee, J.M., Luo, Y., Lupascu, M., Ma, L.N., Marhan, S., Michelsen, A., Mohan, J., Niu, S., Pendall, E., Peñuelas, J., Pfeifer-Meister, L., Poll, C., Reinsch, S., Reynolds, L.L., Schmidt, I.K., Sistla, S., Sokol, N.W., Templer, P.H., Treseder, K.K., Welker, J.M. & Bradford M.A. (2016). Quantifying global soil carbon losses in response to warming. *Nature*, 540(7631), 104–108. DOI: 10.1038/nature20150.
- Dalal, R.C., Thornton, C.M., Allen, D.E. & Kopittke P.M. (2021). A study over 33 years shows that carbon and nitrogen stocks in a subtropical soil are increasing under native vegetation in a changing climate. *Sci. Total Environ.*, 772, 145019. DOI: 10.1016/j.scitotenv.2021.145019.
- De Moraes Sá, J.C., Potma Gonçalves, D.R., Ferreira, L.A., Mishra, U., Inagaki, T.M., Ferreira Furlan, F.J., Moro, R.S., Floriani, N., Briedis, C. & de Oliveira Ferreira A. (2018). Soil carbon fractions and biological activity based indices can be used to study the impact of land management and ecological successions. *Ecological Indicators*, 84, 96–105. DOI: 10.1016/j.ecolind.2017.08.029.
- Doetterl, S., Stevens, A., Six, J., Merckx, R., Oost, K. Van, Pinto, M.C., Casanova-katny, A., Muñoz, C., Boudin, M., Venegas, E.Z. & Boeckx P. (2015). Soil carbon storage controlled by interactions between geochemistry and climate. *Nature Geoscience*, 8(10), 780–783. DOI: 10.1038/ngeo2516.
- Fontaine, S., Barot, S., Barré, P., Bdioui, N., Mary, B. & Rumpel C. (2007). Stability of organic carbon in deep soil layers controlled by fresh carbon supply. *Nature*, 450(7167), 277–280. DOI: 10.1038/nature06275.
- Fu, Y., Taneja, P., Lin, S., Ji, W., Adamchuk, V., Daggupati, P. & Biswas A. (2020). Predicting soil organic matter from cellular phone images under varying soil moisture. *Geoderma*, 361, 114020. DOI: 10.1016/j.geoderma.2019.114020.
- Gholizadeh, A., Saberioon, M., Viscarra Rossel, R.A., Boruvka, L. & Klement A. (2020). Spectroscopic measurements and imaging of soil colour for field scale estimation of soil organic carbon. *Geoderma*, 357, 113972. DOI: 10.1016/j.geoderma.2019.113972.
- Gorban, V.A. (2019). Electrophysical characteristics and dielectric constant of soils of northern natural forests of Ukrainian steppe zone. *Fundamental and Applied Soil Science*, 19(2), 45–50. DOI: 10.15421/041909.
- Gorban, V.A. & Boloban A.O. (2019). Features of the structural-aggregate composition of ordinary chernozems under the steppe and forest vegetation (in Ukrainian). *Ecology and Noospherology*, 30(2), 74–79. DOI: 10.15421/031913.
- Gorban, V., Huslysty, A., Kotovych, O. & Yakovenko V. (2020). Changes in physical and chemical properties of calcic chernozem affected by *Robinia pseudoacacia* and *Quercus robur* plantings. *Ekológia (Bratislava)*, 39(1), 27–44. DOI: 10.2478/eko-2020-0003.
- Gorban, V.A., Khmelenko, O.V., Huslystij, A.O. & Tetiukha O.G. (2019). Influence of forest vegetation on color, reflectivity and humus content in ordinary chernozems (in Ukrainian). *Issues of Steppe Forestry and Forest Reclamation of Soils*, 48, 25–37. DOI: 10.15421/441903.
- Guidelines for soil description (2006). Rome: FAO.
- Günel, H., Erşahin, S., Kutlu, T. & Yetgin B. (2007). Differentiation of soil horizons and parent materials by quantified soil color parameters. *Agrochimica*, 51(1), 86–94.
- Han, P., Dong, D., Zhao, X., Jiao, L. & Lang Y. (2016). A smartphone-based soil color sensor: For soil type classification. *Comput. Electron. Agric.*, 123, 232–241. DOI: 10.1016/j.compag.2016.02.024.
- Horion, S., Ivits, E., De Keersmaecker, W., Tagesson, T., Vogt, J. & Fensholt R. (2019). Mapping European ecosystem change types in response to land-use change, extreme climate events, and land degradation. *Land Degrad. Dev.*, 30(8), 951–963. DOI: 10.1002/ldr.3282.
- IUSS Working Group WRB (2015). *World Reference Base for Soil Resources 2014*, update 2015 International soil classification system for naming soils and creating legends for soil maps.
- Jobbagy, E.G. & Jackson R.B. (2000). The vertical distribution of soil organic carbon and its relation to climate and vegetation. *Ecol. Appl.*, 10, 423–436. DOI: 10.1890/1051-0761(2000)010[0423:TVDOSO]2.0.CO;2.
- Kirillova, N.P., Grauer-Gray, J., Hartemink, A.E., Sileova, T.M., Artemyeva, Z.S. & Burova E.K. (2018). New perspectives to use Munsell color charts with electronic devices. *Comput. Electron. Agric.*, 155, 378–385. DOI: 10.1016/j.compag.2018.10.028.
- Levin, N., Ben-Dor, E. & Singer A. (2005). A digital camera as a tool to measure colour indices and related properties of sandy soils in semi-arid environments. *Int. J. Remote Sens.*, 26(24), 5475–5492. DOI: 10.1080/01431160500099444.
- Li, J., Chen, H. & Zhang C. (2020). Impacts of climate change on key soil ecosystem services and interactions in Central Asia. *Ecological Indicators*, 116, 106490. DOI: 10.1016/j.ecolind.2020.106490.
- Liang, C., Schimel, J.P. & Jastrow J.D. (2017). The importance of anabolism in microbial control over soil carbon storage. *Nature Microbiology*, 2, 17105. DOI: 10.1038/nmicrobiol.2017.105.
- Liles, G.C., Beaudette, D.E., O'Gee, A.T. & Horwath W.R. (2013). Developing predictive soil C models for soils using quantitative color measurements. *Soil Sci. Soc. Am. J.*, 77(6), 2173–2181. DOI: 10.2136/sssaj2013.02.0057.
- Liu, F., Rossiter, D.G., Zhang, G.-L. & Li D.-C. (2020). A soil colour map of China. *Geoderma*, 379, 114556. DOI: 10.1016/j.geoderma.2020.114556.

- López-Díaz, M.L., Benítez, R. & Moreno G. (2017). How do management techniques affect carbon stock in intensive hardwood plantations? *For. Ecol. Manag.*, 389, 228–239. DOI: 10.1016/j.foreco.2016.11.048.
- Ma, X., Zhu, J., Yan, W. & Zhao C. (2020). Assessment of soil conservation services of four river basins in Central Asia under global warming scenarios. *Geoderma*, 375, 114533. DOI: 10.1016/j.geoderma.2020.114533.
- Morellos, A., Pantazi, X.-E., Moshou, D., Alexandridis, T., Whetton, R., Tziotziou, G., Wiebenson, J., Bill, R. & Mouazen A.M. (2016). Machine learning based prediction of soil total nitrogen, organic carbon and moisture content by using VIS-NIR spectroscopy. *Biosystems Engineering*, 152, 104–116. DOI: 10.1016/j.biosystemseng.2016.04.018.
- Moritsuka, N., Matsuoka, K., Katsura, K., Sano, S. & Yanai J. (2014). Soil color analysis for statistically estimating total carbon, total nitrogen and active iron contents in Japanese agricultural soils. *Soil Sci. Plant Nutr.*, 60(4), 475–485. DOI: 10.1080/00380768.2014.906295.
- Nahirniak, S.V., Dontsova, T.A., Lapinsky, A.V., Tereshkov, M.V. & Singh R.C. (2020). Soil and soil breathing remote monitoring: A short review. *Biosystems Diversity*, 28(4), 350–356. DOI: 10.15421/012044.
- Olifir, Y.M., Habryiel, A.J., Partyka, T.V. & Havryshko O.S. (2020). Carbon dioxide emission and humus status of Albic Stagnic Luvisol under different fertilization regimes. *Biosystems Diversity*, 28(3), 320–328. DOI: 10.15421/012040.
- Orlov, D.S., Suchanova, N.I. & Rosanova M.S. (2001). *Spectral reflectance of soils and their components (in Russian)*. Moskva: MSU.
- Pechanec, V., Purkyt, J., Benc, A., Nwaogu, C., Štěrbová, L. & Cudlín P. (2018). Modelling of the carbon sequestration and its prediction under climate change. *Ecological Informatics*, 47, 50–54. DOI: 10.1016/j.ecoinf.2017.08.006.
- Ramos, P.V., Inda, A.V., Barrón, V., Siqueira, D.S., Marques Júnior, J. & Teixeira D.D.B. (2020). Color in subtropical brazilian soils as determined with a Munsell chart and by diffuse reflectance spectroscopy. *Catena*, 193, 104609. DOI: 10.1016/j.catena.2020.104609.
- Recio Espejo, J.M., Kotovych, O.V., Díaz del Olmo, F., Gorban, V.A., Cámara Artigas, R., Masyuk, O.M. & Borja Barrera C. (2020). Palaeoecological aspects of an Ukrainian Upper Holocene chernozem. *Ecology and Nospherology*, 31(2), 59–64. DOI: 10.15421/032009.
- Rodríguez Martín, J.A., Álvaro-Fuentes, J., Gonzalo, J., Gil, C., Ramos-Miras, J.J., Grau Corbí, J.M. & Boluda R. (2016). Assessment of the soil organic carbon stock in Spain. *Geoderma*, 264, 117–125. DOI: 10.1016/j.geoderma.2015.10.010.
- Sánchez-Marañón, M., Soriano, M., Melgosa, M., Delgado, G. & Delgado R. (2004). Quantifying the effects of aggregation, particle size and components on the colour of Mediterranean soils. *Eur. J. Soil Sci.*, 55(3), 551–565. DOI: 10.1111/j.1365-2389.2004.00624.x.
- Simón, T., Zhang, Y., Hartemink, A.E., Huang, J., Walter, C. & Yost J. L. (2020). Predicting the color of sandy soils from Wisconsin, USA. *Geoderma*, 361, 114039. DOI: 10.1016/j.geoderma.2019.114039.
- Swetha, R.K. & Chakraborty S. (2021). Combination of soil texture with Nix color sensor can improve soil organic carbon prediction. *Geoderma*, 382, 114775. DOI: 10.1016/j.geoderma.2020.114775.
- Taneja, P., Vasava, H.K., Daggupati, P. & Biswas A. (2021). Multi-algorithm comparison to predict soil organic matter and soil moisture content from cell phone images. *Geoderma*, 385, 114863. DOI: 10.1016/j.geoderma.2020.114863.
- Torrent, J. & Barrón V. (2015). Diffuse reflectance spectroscopy. In A.L. Ulery & R.L. Drees (Eds.), *Methods soil analysis, mineralogical methods* (pp. 367–385). SSSA Book Series. DOI: 10.2136/sssabookser5.5.c13.
- Trigalet, S., Gabarrón-Galeote, M.A., Van Oost, K. & van Wesemael B. (2016). Changes in soil organic carbon pools along a chronosequence of land abandonment in southern Spain. *Geoderma*, 268, 14–21. DOI: 10.1016/j.geoderma.2016.01.014.
- Wu, C., Yang, Y. & Xia J. (2017). A simple digital imaging method for estimating black-soil organic matter under visible spectrum. *Archives of Agronomy and Soil Science*, 63(10), 1346–1354. DOI: 10.1080/03650340.2017.1280728.
- Yakovenko, V. (2017). Fractal properties of coarse/fine-related distribution in forest soils on colluvium. In D. Dent & Y. Dmytruk (Eds.), *Soil science working for a living* (pp. 29–42). Switzerland: Springer International Publishing. DOI: 10.1007/978-3-319-45417-7.
- Zhou, P., Li, M.-Z., Yang, W., Ji, R.-H. & Meng C. (2020). Development of Vehicle-Mounted in-situ soil parameters detector based on NIR Diffuse Reflection. *Guang Pu Xue Yu Guang Pu Fen Xi/Spectroscopy and Spectral Analysis*, 40(9), 2856–2861. DOI: 10.3964/j.issn.1000-0593(2020)09-2856-06.